

Terahertz Vibration–Rotation–Tunneling Spectroscopy of the Ammonia Dimer: Characterization of an out of Plane Vibration

Wei Lin, Jia-Xiang Han, Lynelle K. Takahashi, Jennifer G. Loeser,[†] and Richard J. Saykally*

Department of Chemistry, University of California, Berkeley, California 94720

Received: January 26, 2006; In Final Form: March 26, 2006

The terahertz vibration–rotation–tunneling (VRT) spectrum of the ammonia dimer (NH₃)₂ has been measured between ca. 78.5 and 91.9 cm⁻¹. The dipole-allowed transitions are separated into three groups that correspond to the 3-fold internal rotation of the NH₃ subunits. Transitions have been assigned for VRT states of the A–A (ortho–ortho) combinations of NH₃ monomer states. The spectrum is further complicated by strong Coriolis interactions. $K = 0 \leftarrow 0$, $K = 1 \leftarrow 0$, $K = 0 \leftarrow 1$, and $K = 1 \leftarrow 1$ progressions have been assigned. The band origins, rotational constants, asymmetry doubling, centrifugal distortion, and Coriolis coupling constant have been determined from the fit to an effective Hamiltonian. These VRT transitions are tentatively assigned to an out of plane vibration with a $K = 0$ state at 89.141305(47) cm⁻¹, and a $K = 1$ state at 86.77785(9) cm⁻¹.

Introduction

As one of the three textbook prototypes of hydrogen bonding, ammonia has received a great deal of attention from both theory and experiment.¹ The ammonia dimer has been of particular interest to both the high-resolution spectroscopy and ab initio communities as a result of efforts to quantify the nature of ammonia hydrogen bonds. Nelson et al.^{2–4} published their pioneering microwave molecular beam studies of several dimer isotopomers in 1985 and 1987, wherein they concluded that the dimer was quasi-rigid, with a cyclic hydrogen bond geometry. This conclusion strongly contrasted with the traditional view of linear hydrogen bonds in ammonia established from both matrix spectroscopy⁵ and theoretical calculations^{6,7} and engendered a vigorous debate that continues to the present.⁸ Havenith et al.⁹ subsequently measured six tunneling subbands near 25 cm⁻¹ by tunable far-infrared laser spectroscopy, and later three more subbands¹⁰ using infrared–far-infrared double resonance. In a comprehensive study of the dimer ground vibrational state, Loeser et al.¹¹ measured $A + A$ VRT states with $j = k = 0$ and $j = k = 1$ levels between 0 and 25 cm⁻¹ above the lowest energy $A + A$ state, $A + E$ VRT states with $j = k = 0$, $j = k = 1$ and $j = k = 2$ levels between 0 and 40 cm⁻¹ above the lowest energy $A + E$ state, and $E + E$ VRT with $j = k = 0$, $j = k = 1$, and $j = k = 2$ levels between 0 and 40 cm⁻¹ above the lowest energy $E + E$ state. Both that work and the infrared–far-infrared double resonance work by Havenith et al.¹⁰ unambiguously established that the tunneling states observed by Nelson et al. were actually the umbrella inversion states of the ammonia monomers in the complex. Moreover, it was concluded that the dimer is actually extremely nonrigid, in contrast to the conclusion of Nelson et al. This had the effect of invalidating their structural determination that was based on inversion of Legendre polynomials in the polar angles, since this approach is only appropriate for fairly rigid systems. Later on, Linnartz et al.¹² performed a far-IR Stark experiment, in which they determined the dipole moment of the 487 GHz band ($K = 1$) G state to be 0.10 D for the ground

state and established an upper limit of 0.09D for the dipole moment of the excited $K = 1$ G state. Cotti et al.¹³ performed a far-IR Stark experiment of the 747 GHz band ($K = -1$) G state and determined the dipole moments to be 0.763(15) and 0.365(10) D for the ground and excited states, respectively. These values vary substantially from the value of 0.74 D of the ($K = 0$) G state reported by Nelson et al.³. Such a strong variation of the dipole moment with quantum state further evidences the highly nonrigid nature of this complex. Heineking et al.¹⁴ analyzed the ¹⁴N nuclear hyperfine structure of some rotation–inversion transitions in the lowest $K = 1$ E₃ state. Behrens et al.¹⁵ studied the infrared molecular beam depletion spectrum of the ammonia dimer in cold helium clusters, in which they found that the dominating interchange tunnelings in free ammonia dimers are largely quenched in a superfluid helium cluster at 0.4 K. Finally, Karyakin et al.¹⁶ measured the millimeter and submillimeter-wave molecular beam spectrum of the $A + A$ state of (ND₃)₂. Müller-Dethlefs and Hobza¹⁷ used the ammonia dimer as an illustrative example in their review article on noncovalent interactions. Havenith¹⁸ recently reviewed the experimental studies of the ammonia dimer. Bunker and Jensen¹⁹ discussed the ammonia dimer in their book on molecular symmetry and spectroscopy.

In addition to these experimental studies, there has also been a substantial number of theoretical investigations of this system,²⁰ with over 36 papers appearing since the Loeser et al. work. Perhaps of most relevance to the spectroscopic studies, Olthof et al.^{21,22} carried out fully coupled six dimensional dynamical calculations on a model intermolecular potential energy surface (IPS). That work provided the essential quantitative link between theoretical intermolecular potential energy surfaces for the ammonia dimer and the experimental far-infrared spectrum, microwave spectrum, dipole moment measurements, and average angles determined from the ¹⁴N quadrupole coupling constants. With this work, the debate on the ammonia dimer seemed resolved.²³ Due to the extreme floppiness of ammonia dimer, vibrational averaging plays a crucial role in the experimentally determined properties. All of the modern high level theoretical calculations agree that the potential energy surface is extremely flat, such that the debate

* Corresponding author. E-mail: Saykally@berkeley.edu.

[†] Current address: Department of Chemistry, College of Marin, Kentfield, CA 94904.

as to whether the hydrogen bond is linear or bent is no longer meaningful insofar as the hydrogen bonding properties are concerned.

In fact, high-resolution VRT spectra of the ammonia dimer reveal complicated splitting patterns for vibration–rotation transitions that result from large-amplitude tunneling motions. These tunneling dynamics can be derived from spectral splittings and shifts, and provide a very sensitive test of a given potential energy surface. Loeser et al.¹¹ established the tunneling dynamics for the ground vibrational states from the VRT spectra. The interchange tunneling motion has the lowest energy barrier among the tunneling dynamics, interchanging the role of the donor and acceptor monomers. The barrier was calculated by Olthof et al.²¹ to be only 7 cm^{-1} . The interchange splittings were directly determined from the VRT spectra of the ground state. The observed interchange splittings are 16.1 cm^{-1} for the $K = 0 \leftarrow 0\text{ } A-A$ (ortho–ortho) subband, 20.5 cm^{-1} for the $K = 0 \leftarrow 0\text{ } A-E$ (ortho–para) subband, and 19.3 cm^{-1} for the $K = 0 \leftarrow 0\text{ } E-E$ (para–para) subband. The splittings due to internal rotation cannot be determined by experimental data alone. Behrens et al.¹⁵ estimated this quantity to be on the order of 1–10 GHz. The least significant tunneling dynamics are the monomer (para) umbrella inversion splittings. For the $K = 0$ tunneling sublevels, the first-order para monomer inversion splitting of the $A-E$ (ortho–para) states is 3.3 GHz in the lower state and 2.4 GHz in the upper state. These values are much smaller than the splitting (23.8 GHz) for the ammonia monomer, which suggests that the inversion is substantially hindered.

With a total potential energy well depth of 1020 cm^{-1} for the IPS, Olthof et al. predicted that the dissociation energies of the lowest $A + A$, $A + E$, and $E + E$ states are 639, 635, and 631 cm^{-1} , respectively. In recent years, the Berkeley terahertz laser spectrometer has been successfully used in studies of the water dimer,²⁴ trimer,^{25,26} and larger clusters up to hexamer,^{27,28} and several versions of the water dimer IPS have been determined.^{29–31} To proceed toward the goal of determining a more accurate IPS for the ammonia dimer, it is necessary to quantitatively characterize the intermolecular vibrations using this same approach.

Here we present the measurement and assignment of the VRT spectrum of $(\text{NH}_3)_2$ dimer for an out-of-plane vibration correlating asymptotically to A -symmetry monomer rovibrational states. A preliminary account was given by Loeser et al.³² Measurements were made for both $K = 0$ and $K = 1$, and the spectra are complicated by Coriolis interactions between these states. These effects are similar to those previously observed in lower $(\text{NH}_3)_2$ states, which aids in making the assignments. About 500 individual transitions were assigned for this out-of-plane vibration, and the fitting of the more complex $A-E$ (ortho–para) and $E-E$ (para–para) states is ongoing.

An initial estimate of the ordering of the tunneling sublevels for an intermolecular vibrational mode of $(\text{NH}_3)_2$ can be obtained by multiplying the symmetries of the ground-state tunneling sublevels by the symmetry of the intermolecular vibration. This does not take into account the possible reordering resulting from large changes in the tunneling frequency affected by vibrational excitation. We will here assume that the ordering of the tunneling frequencies (interchange $>$ internal rotation $>$ umbrella inversion) is not changed in the excited intermolecular vibration states. Then, the ordering of the tunneling sublevels in the three in-plane vibrations, which have A' symmetry in C_s , is expected to be the same as in the ground state. The stretch and “cis” in-plane bend has A_4 symmetry in \mathbf{G}_{36} , and has a double well potential. Of the out-of-plane vibrations, which have

TABLE 1: Harmonic Frequencies (cm^{-1}) for the Intermolecular Vibrational Modes of the Ammonia Dimer from Several *ab Initio* and Model Potential Energy Surfaces

	ref 33	ref 34	ref 6	ref 35	pseudodiatomic model
A' Modes					
trans in-plane bend	72	81	100	121	71 ^a
stretch	138	160	128	166	107
cis in-plane bend	393	334	392	444	239 ^a
A'' Modes					
antigeared twist	35	27	12	20	
geared twist	114	120	112	137	
out-of-plane torsion	257	186	247	293	171 ^a

^a The $(\text{HCl})_2$ bending vibrational frequencies, calculated exactly from the experimentally determined potential from ref 35.

A'' symmetry in C_s , the out-of-plane torsion in γ and the “anti-geared” out-of-plane twist, both have A_3 symmetry in \mathbf{G}_{36} . For these modes, the lower $K = 0$ interchange tunneling sublevels will be A_3 , G , E_2 , and E_3 and the upper $K = 0$ interchange tunneling sublevels will be A_2 , G , E_1 , and E_4 . The “geared” out-of-plane twist has A_2 symmetry in \mathbf{G}_{36} , so that the lower and upper interchange tunneling sublevels will be exchanged with respect to the A_3 ordering.

To date, the only estimates for the ammonia dimer intermolecular vibrational frequencies come from harmonic approximation analyses of various potential energy surfaces. Table 1 lists harmonic frequencies for the intermolecular modes of the ammonia dimer from the theoretical work of Marsden,³³ Dykstra and Andrews,³⁴ who also provide double harmonic estimates for the transition dipoles from the ground state to the intermolecular modes of the ammonia dimer, and Frisch et al.⁶ None of these authors provide descriptions of the modes they calculated beyond the A' and A'' symmetry labels in C_s and the intermolecular stretch, so the mode descriptions given in Table 1 are only estimated. Since the HCl monomer has a B rotational constant similar to that of the NH_3 monomer, and since both dimers are known to have similarly large interchange frequencies, the $(\text{HCl})_2$ bending vibrational frequencies, calculated exactly from the experimentally determined potential of Elrod et al.³⁵ are given in Table 1 for comparison.

For the intermolecular stretch, the pseudodiatomic approximation, using the ground-state rotational constants of the ammonia dimer, may yield a useful estimate. In the pseudodiatomic approximation

$$\nu_{\text{stretch}} \approx \sqrt{\frac{4B^3}{D}}$$

This yields $\sim 106\text{--}107\text{ cm}^{-1}$ for the unperturbed ground-state tunneling sublevels.

Because of the large tunneling splittings, the complete observation of a single intermolecular vibration requires several far-infrared (FIR) laser lines. The measurement of these spectra at higher frequencies is currently limited by the availability of strong far-IR laser lines.

Experimental Section

The Berkeley terahertz laser spectrometer, which has been described in detail elsewhere,^{36,37} was used to measure absorption spectra of the ammonia dimer in the 2.35–3.2 THz range. The clusters were formed by continuously expanding 1–2 atm of a 0.5–1% mixture of NH_3 in Ar through a 4 in. \times 0.005 in. slit nozzle. The resulting beam temperature was ca. 4 K. The continuous planar expansion was positioned in the center of a Perry (multipass) cell, where the tunable terahertz sidebands

intersected it eight times before being detected by a stressed Ga:Ge photoconductor. The 2409.2932 GHz (*trans*-CH₂F₂) far-infrared laser was mixed with microwave radiation between 6 and 56 GHz, and the 2447.9685 (CD₃OH) (± 40), 2522.7815 (CH₃OH) (± 40), 2546.4950 (*trans*-CH₂F₂) (± 40), 2633.8991 (¹³CH₃OH) (± 40), and 2714.7151 GHz (¹³CH₃OH) (± 40) lasers were mixed with microwave radiation between 6 and 40 GHz to provide extensive spectral coverage between 78.5 and 91.9 cm⁻¹. The scanning sensitivity was reduced for microwave frequencies below 12.3 GHz because the optimum FM modulation depth (~ 1.5 MHz) is not available from the microwave synthesizer for these frequencies. Atmospheric H₂O absorptions, especially those at 2365.8997 (3₃₁ \leftarrow 3₂₂), 2391.5730 (4₀₄ \leftarrow 3₁₃), 2362.9331 (4₃₂ \leftarrow 4₂₃), and 2340.4740 (4₁₄ \leftarrow 3₀₃), as well as the laser gaps of the 2409, 2634, and 2715 GHz lasers restricted the otherwise continuous spectral coverage.

Analysis and Discussion

A total of more than 700 transitions were recorded. Among them about 500 were assigned to the ammonia dimer; 59 of these were assigned to the two *A* + *A* vibration-rotation-tunneling states of this excited vibrational state based upon ground-state combination differences. One each of the $K = 0 \leftarrow 0$, $K = 1 \leftarrow 0$, $K = 0 \leftarrow 1$, and $K = 1 \leftarrow 1$ progressions was assigned. These transitions involve two new excited states: a $K = 0$ stack of B_2^- symmetry 2672.4 GHz above the lowest $K = 0$ *A* + *A* state and a $K = 1$ stack of B_2^-/A_2^+ symmetry 2601.5 GHz above the lowest $K = 0$ *A* + *A* state. Loeser et al.¹¹ demonstrated that the G_{144} instead of G_{36} molecular symmetry group should be used when the monomer inversion is involved. For the G_{144} molecular symmetry group, the selection rules for these transitions are $A_2^+ \leftrightarrow A_2^-$ and $B_2^+ \leftrightarrow B_2^-$. These transitions are listed in Table 2 along with their assigned quantum numbers and symmetries. The strongest transitions are in the *b*-type $K = 1 \leftarrow 0$ and $K = 0 \leftarrow 1$ subbands, and they exhibit a signal-to-noise ratio of up to 120.

The assigned transitions were fit to an effective pseudolinear energy level expression using SPFIT.³⁸

$$E = E_n + B_n J(J+1) - D_n (J(J+1))^2 \quad (1)$$

$$E = E_n + B_n (J(J+1) - K^2) - D_n (J(J+1) - K^2)^2 \pm q_B J(J+1) \pm q_D [J(J+1)]^2 \quad (2)$$

where B is the rotational constant, D is the centrifugal distortion constant, and n is the state number. q_B represents the parity doubling constant corresponding to asymmetry doubling, which is constrained to be positive in the fit. q_D is the associated centrifugal distortion term. We use expression 1 for the $K = 0$ manifold and expression 2 for the $K = 1$ manifold. Since we essentially treat VRT states with different K_a values as different vibrational states, when the perturbation is absent, the $K = 1$ levels appear to have an "asymmetry" doubling effect. When the Coriolis interaction was strongly perturbing, as is the case for this out-of-plane vibration, a Coriolis coupling constant c ($= 2\sqrt{2} B\zeta$) was used to account for the off-diagonal matrix elements between the two VRT levels of the same J and the same symmetry with $K = 0$ and $K = 1$.

A combined fit was performed using these transitions and the previously assigned rotation-tunneling transitions (which are also listed in Table 2) involving the VRT state of the same *A*–*A* (ortho–ortho) state. The experimental error for the measured frequencies was 1 MHz for previously measured transitions and 2 MHz for the new terahertz transitions in the fit. All the

transitions were weighted equally. The standard deviations of the fit to the vibration-rotation-tunneling transitions only and for the combined fit are both about 1.2 MHz. The spectroscopic constants resulting from the fit are given in Table 3. The first column lists the constants from the fit of the 59 new THz transitions, the second column gives the constants resulting from the overall combined fit. The values from previous analyses are also listed for comparison. Figure 1 shows the recorded spectrum of the measured THz transitions, and Figure 2 shows the spectrum for the *A*–*A* (ortho–ortho) state, while Figure 3 gives the summary energy level diagram of the assigned VRT states of the *A*–*A* (ortho–ortho) state.

In the vibrationally excited state of (NH₃)₂, the difference between the energy of $K = 1$ and $K = 0$ states is only 71 GHz, which implies strong Coriolis coupling. The Coriolis coupling constant between the $K = 1$ and $K = 0$ states is determined to be 6460 (46) MHz. Loeser et al.¹¹ were able to fit the *A*–*A* ground states with only the asymmetry doubling constant, analogous to the q parameter used here. This is also much larger than that of the *A*–*E* ground states, indicating a much stronger Coriolis interaction between the $K = 0$ and $K = 1$ states. This Coriolis interaction also results in the observation of an otherwise forbidden $K = 0 \leftarrow 0$ Q branch. In addition, even though (NH₃)₂ is a near-prolate top, the $K = 1$ manifold lies almost 71 GHz below the $K = 0$ manifold, while in the ground state the lowest *A* + *A* $K = 1$ manifold lies 210 GHz above the lowest $K = 0$ manifold. This indicates that K_a is a poor quantum number in this out-of-plane intermolecular vibration than in the ground state, or proposes that there is vibrational angular momentum directed along the *a*-axis of the dimer in what is normally a $K_a = 0$ state. The states with the same overall symmetry are allowed to mix if they have the same J rotational quantum number. This Coriolis interaction results in characteristic shifts of all the transitions involving the $K = 0$ manifold and half of the asymmetry doublets of the $K = 1$ manifold. The net result is that the two sets of energy levels shift further apart, with $K = 0$ manifold being lower and $K = 1$ manifold above. It should also be noted that in a floppy molecule like the ammonia dimer, K_c is not a good quantum number either and labeling of levels as K -type doubling components is not strictly correct.³⁹

We have also measured many transitions for VRT states of dimers having *A* + *E* and *E* + *E* monomer progenitors. At present, the assignment of these complex spectra is incomplete, but indicative of strong Coriolis interactions between the $K = 0$ and $K = 1$ components of the dimer state.⁴⁰ Further measurements will be required to complete the analysis.

From the analysis of *A* + *A* state and the initial assignment of *A* + *E* and *E* + *E* states, it appears that we have observed only half of the interchange tunneling sublevels. From partial analysis of the *E* + *E* state, we believe that these are the lower interchange levels of an out-of-plane vibration, which must therefore have A_3 symmetry in G_{36} . Two of the three out-of-plane modes described in the Introduction have A_3 symmetry in G_{36} , the out-of-plane torsion and the "antigear" out-of-plane twist. Some motion in the dihedral angle must be invoked to give the change in dipole necessary for the observation of this mode. The observed vibration may be too low in frequency for it to be the analogue of (HCl)₂ out-of-plane torsion which occurs at 171 cm⁻¹ and is predicted to be roughly the same for (NH₃)₂. This suggests that the observed mode involves the out-of-plane twist, which can be mixed by the potential with the out-of-plane torsion. The harmonic frequencies for the lowest

TABLE 2: Measured Frequencies for the A–A (Ortho–Ortho) Transitions of (NH₃)₂^a

<i>J'</i>	sym'	<i>K'</i>	<i>n'</i>	<i>J''</i>	sym''	<i>K''</i>	<i>n''</i>	freq (MHz)	obsd – calcd	<i>J'</i>	sym'	<i>K'</i>	<i>n'</i>	<i>J''</i>	sym''	<i>K''</i>	<i>n''</i>	freq (MHz)	obsd – calcd
15	B ₂ ⁻	0	4	14	B ₂ ⁺	0	1	611720.0	0.2	8	B ₂ ⁻	1	5, 6	7	B ₂ ⁺	1	2, 3	592089.0	0.3
14	A ₂ ⁺	0	4	13	A ₂ ⁻	0	1	604642.5	-0.4	9	B ₂ ⁻	1	5, 6	8	B ₂ ⁺	1	2, 3	602013.1	-0.3
13	B ₂ ⁻	0	4	12	B ₂ ⁺	0	1	597359.1	-0.0	9	A ₂ ⁺	1	5, 6	8	A ₂ ⁻	1	2, 3	600206.8	-0.7
12	A ₂ ⁺	0	4	11	A ₂ ⁻	0	1	589867.0	0.3	10	B ₂ ⁻	1	5, 6	9	B ₂ ⁺	1	2, 3	608090.4	1.9
9	B ₂ ⁻	0	4	8	B ₂ ⁺	0	1	566121.0	-0.3	10	A ₂ ⁺	1	5, 6	9	A ₂ ⁻	1	2, 3	610275.4	-0.3
8	A ₂ ⁺	0	4	7	A ₂ ⁻	0	1	557778.8	-0.6	11	A ₂ ⁺	1	5, 6	10	A ₂ ⁻	1	2, 3	615735.6	2.4
7	B ₂ ⁻	0	4	6	B ₂ ⁺	0	1	549222.6	-0.1	11	B ₂ ⁻	1	5, 6	10	B ₂ ⁺	1	2, 3	618335.2	0.5
6	A ₂ ⁺	0	4	5	A ₂ ⁻	0	1	540450.3	-0.4	12	B ₂ ⁻	1	5, 6	11	B ₂ ⁺	1	2, 3	623141.2	-2.1
5	B ₂ ⁻	0	4	4	B ₂ ⁺	0	1	531462.8	-0.4	12	A ₂ ⁺	1	5, 6	11	A ₂ ⁻	1	2, 3	626191.3	0.2
4	A ₂ ⁺	0	4	3	A ₂ ⁻	0	1	522259.7	-0.3	13	B ₂ ⁻	1	5, 6	12	B ₂ ⁺	1	2, 3	633845.7	0.0
3	B ₂ ⁻	0	4	2	B ₂ ⁺	0	1	512841.1	-0.4	1	A ₂ ⁺	1	5, 6	1	A ₂ ⁻	1	2, 3	518251.6	-0.3
2	A ₂ ⁺	0	4	1	A ₂ ⁻	0	1	503207.7	-0.4	1	B ₂ ⁻	1	5, 6	1	B ₂ ⁺	1	2, 3	518312.3	-0.1
1	B ₂ ⁻	0	4	0	B ₂ ⁺	0	1	493359.8	-0.7	2	B ₂ ⁻	1	5, 6	2	B ₂ ⁺	1	2, 3	517756.0	1.4
0	A ₂ ⁺	0	4	1	A ₂ ⁻	0	1	473026.8	0.3	3	A ₂ ⁺	1	5, 6	3	A ₂ ⁻	1	2, 3	517008.7	-0.4
1	B ₂ ⁻	0	4	2	B ₂ ⁺	0	1	462543.2	0.4	4	B ₂ ⁻	1	5, 6	4	B ₂ ⁺	1	2, 3	516015.9	-0.4
2	A ₂ ⁺	0	4	3	A ₂ ⁻	0	1	451850.0	0.0	7	A ₂ ⁺	0	9	8	A ₂ ⁻	1	2, 3	2400641	-1.8
3	B ₂ ⁻	0	4	4	B ₂ ⁺	0	1	440949.4	-0.6	4	B ₂ ⁻	0	9	5	B ₂ ⁺	1	2, 3	2418607	-1.6
4	A ₂ ⁺	0	4	5	A ₂ ⁻	0	1	429846.2	1.2	3	A ₂ ⁺	0	9	4	A ₂ ⁻	1	2, 3	2425741	1.7
5	B ₂ ⁻	0	4	6	B ₂ ⁺	0	1	418538.3	1.0	2	B ₂ ⁻	0	9	3	B ₂ ⁺	1	2, 3	2433567	-0.3
6	A ₂ ⁺	0	4	7	A ₂ ⁻	0	1	407030.2	0.7	1	A ₂ ⁺	0	9	2	A ₂ ⁻	1	2, 3	2442165	1.0
7	B ₂ ⁻	0	4	8	B ₂ ⁺	0	1	395324.8	0.3	0	B ₂ ⁻	0	9	1	B ₂ ⁺	1	2, 3	2451586	0.8
8	A ₂ ⁺	0	4	9	A ₂ ⁻	0	1	383425.3	-0.0	4	B ₂ ⁻	0	9	4	B ₂ ⁺	1	2, 3	2469853	1.4
8	A ₂ ⁺	1	5, 6	9	A ₂ ⁻	0	1	630121.2	0.1	5	A ₂ ⁺	0	9	5	A ₂ ⁻	1	2, 3	2473540	-0.6
7	B ₂ ⁻	1	5, 6	8	B ₂ ⁺	0	1	641805.8	0.5	6	B ₂ ⁻	0	9	6	B ₂ ⁺	1	2, 3	2477755	0.6
6	A ₂ ⁺	1	5, 6	7	A ₂ ⁻	0	1	653322.8	0.6	7	A ₂ ⁺	0	9	7	A ₂ ⁻	1	2, 3	2482422	0.7
5	B ₂ ⁻	1	5, 6	6	B ₂ ⁺	0	1	664669.2	0.6	8	B ₂ ⁻	0	9	8	B ₂ ⁺	1	2, 3	2487478	1.6
4	A ₂ ⁺	1	5, 6	5	A ₂ ⁻	0	1	675842.2	0.5	9	A ₂ ⁺	0	9	9	A ₂ ⁻	1	2, 3	2492859	-2.5
3	B ₂ ⁻	1	5, 6	4	B ₂ ⁺	0	1	686839.4	0.7	2	B ₂ ⁻	0	9	1	B ₂ ⁺	1	2, 3	2484942	0.4
2	A ₂ ⁺	1	5, 6	3	A ₂ ⁻	0	1	697658.5	0.8	3	A ₂ ⁺	0	9	2	A ₂ ⁻	1	2, 3	2497653	-0.3
1	B ₂ ⁻	1	5, 6	2	B ₂ ⁺	0	1	708297.3	1.8	4	B ₂ ⁻	0	9	3	B ₂ ⁺	1	2, 3	2511052	-0.5
1	B ₂ ⁻	1	5, 6	0	B ₂ ⁺	0	1	739115.1	0.1	5	A ₂ ⁺	0	9	4	A ₂ ⁻	1	2, 3	2525059	-0.3
2	A ₂ ⁺	1	5, 6	1	A ₂ ⁻	0	1	749016.8	-1.3	6	B ₂ ⁻	0	9	5	B ₂ ⁺	1	2, 3	2539597	1.5
3	B ₂ ⁻	1	5, 6	2	B ₂ ⁺	0	1	758731.2	0.4	7	A ₂ ⁺	0	9	6	A ₂ ⁻	1	2, 3	2554588	-0.3
4	A ₂ ⁺	1	5, 6	3	A ₂ ⁻	0	1	768257.6	-0.3	9	B ₂ ⁻	0	9	8	B ₂ ⁺	1	2, 3	2585688	1.2
5	B ₂ ⁻	1	5, 6	4	B ₂ ⁺	0	1	777595.4	0.3	8	A ₂ ⁺	1	7, 8	9	A ₂ ⁻	0	1	2509969	-1.6
6	A ₂ ⁺	1	5, 6	5	A ₂ ⁻	0	1	786744.4	0.2	7	B ₂ ⁻	1	7, 8	8	B ₂ ⁺	0	1	2518951	-1.7
7	B ₂ ⁻	1	5, 6	6	B ₂ ⁺	0	1	795704.5	-0.2	6	A ₂ ⁺	1	7, 8	7	A ₂ ⁻	0	1	2528062	-0.8
8	A ₂ ⁺	1	5, 6	7	A ₂ ⁻	0	1	804475.8	-2.5	5	B ₂ ⁻	1	7, 8	6	B ₂ ⁺	0	1	2537316	1.2
9	B ₂ ⁻	1	5, 6	8	B ₂ ⁺	0	1	813058.7	-0.4	4	A ₂ ⁺	1	7, 8	5	A ₂ ⁻	0	1	2546720	-0.4
10	A ₂ ⁺	1	5, 6	9	A ₂ ⁻	0	1	821453.8	-0.4	3	B ₂ ⁻	1	7, 8	4	B ₂ ⁺	0	1	2556288	-1.2
11	B ₂ ⁻	1	5, 6	10	B ₂ ⁺	0	1	829661.8	-0.4	2	A ₂ ⁺	1	7, 8	3	A ₂ ⁻	0	1	2566029	0.5
12	A ₂ ⁺	1	5, 6	11	A ₂ ⁻	0	1	837683.8	0.5	1	B ₂ ⁻	1	7, 8	2	B ₂ ⁺	0	1	2575945	1.5
1	A ₂ ⁺	1	5, 6	1	A ₂ ⁻	0	1	728792.5	-0.9	1	B ₂ ⁻	1	7, 8	0	B ₂ ⁺	0	1	2606762	0.8
2	B ₂ ⁻	1	5, 6	2	A ₂ ⁻	0	1	728323.5	0.5	2	A ₂ ⁺	1	7, 8	1	A ₂ ⁻	0	1	2617388	1.4
3	A ₂ ⁺	1	5, 6	3	A ₂ ⁻	0	1	727620.7	-1.6	5	B ₂ ⁻	1	7, 8	4	B ₂ ⁺	0	1	2650243	2.4
4	B ₂ ⁻	1	5, 6	4	B ₂ ⁺	0	1	726684.9	-1.4	6	A ₂ ⁺	1	7, 8	5	A ₂ ⁻	0	1	2661485	1.0
5	A ₂ ⁺	1	5, 6	5	A ₂ ⁻	0	1	725517.2	1.0	7	B ₂ ⁻	1	7, 8	6	B ₂ ⁺	0	1	2672852	1.1
6	B ₂ ⁻	1	5, 6	6	B ₂ ⁺	0	1	724119.1	-1.4	8	A ₂ ⁺	1	7, 8	7	A ₂ ⁻	0	1	2684322	-2.7
7	A ₂ ⁺	1	5, 6	7	A ₂ ⁻	0	1	722492.1	-0.4	9	B ₂ ⁻	1	7, 8	8	B ₂ ⁺	0	1	2695889	2.6
8	B ₂ ⁻	1	5, 6	8	B ₂ ⁺	0	1	720638.4	-1.4	1	A ₂ ⁺	1	7, 8	1	A ₂ ⁻	0	1	2595937	1.1
9	A ₂ ⁺	1	5, 6	9	A ₂ ⁻	0	1	718560.0	1.1	2	B ₂ ⁻	1	7, 8	2	B ₂ ⁺	0	1	2595217	0.1
10	B ₂ ⁻	1	5, 6	10	B ₂ ⁺	0	1	716259.5	0.8	3	A ₂ ⁺	1	7, 8	3	A ₂ ⁻	0	1	2594207	1.2
11	A ₂ ⁺	1	5, 6	11	A ₂ ⁻	0	1	713739.7	-0.8	4	B ₂ ⁻	1	7, 8	4	B ₂ ⁺	0	1	2592969	1.1
4	B ₂ ⁻	1	5, 6	5	B ₂ ⁺	1	2, 3	464773.3	-1.0	5	A ₂ ⁺	1	7, 8	5	A ₂ ⁻	0	1	2591573	0.8
4	A ₂ ⁺	1	5, 6	5	A ₂ ⁻	1	2, 3	465101.9	-0.6	6	B ₂ ⁻	1	7, 8	6	B ₂ ⁺	0	1	2590085	1.7
3	A ₂ ⁺	1	5, 6	4	A ₂ ⁻	1	2, 3	475984.0	-0.9	7	A ₂ ⁺	1	7, 8	7	A ₂ ⁻	0	1	2588561	2.8
3	B ₂ ⁻	1	5, 6	4	B ₂ ⁺	1	2, 3	476170.8	-0.6	9	A ₂ ⁺	1	7, 8	9	A ₂ ⁻	0	1	2585583	1.9
2	B ₂ ⁻	1	5, 6	3	B ₂ ⁺	1	2, 3	486964.2	-3.1	10	B ₂ ⁻	1	7, 8	10	B ₂ ⁺	0	1	2584198	0.2
2	A ₂ ⁺	1	5, 6	3	A ₂ ⁻	1	2, 3	487046.9	0.2	11	A ₂ ⁺	1	7, 8	11	A ₂ ⁻	0	1	2582917	-0.2
1	A ₂ ⁺	1	5, 6	2	A ₂ ⁻	1	2, 3	497711.6	-0.3	4	B ₂ ⁻	0	9	4	B ₂ ⁺	0	1	2680519	-1.0
1	B ₂ ⁻	1	5, 6	2	B ₂ ⁺	1	2, 3	497728.3	0.2	3	A ₂ ⁺	0	9	3	A ₂ ⁻	0	1	2677375	-0.8
2	B ₂ ⁻	1	5, 6	1	B ₂ ⁺	1	2, 3	538338.5	0.2	2	B ₂ ⁻	0	9	2	B ₂ ⁺	0	1	2674925	-1.4
2	A ₂ ⁺	1	5, 6	1	A ₂ ⁻	1	2, 3	538476.1	0.1	6	B ₂ ⁻	0	9	6	B ₂ ⁺	0	1	2688581	-0.1
3	B ₂ ⁻	1	5, 6	2	B ₂ ⁺	1	2, 3												

TABLE 3: Spectroscopic Constants for the A–A (Ortho–Ortho) States of the Ammonia Dimer

state	param	this work	combined fit	ref 11	ref 9	ref 10
1	B/MHz	5136.626 (56)	5136.636 (24)	5136.646 (31)	5136.517 (97)	5136.601 (13)
	D/kHz	58.21 (51)	58.74 (23)	58.92 (29)	39.49(42)	58.53 (34)
2, 3	$E_{2,3}/\text{MHz}$	215668.96 (81)	215667.18 (38)	210526.08 (49) ^a		
	B/MHz	5140.918 (64)	5140.865 (27)	5140.986 (34)		
	D/kHz	56.69 (64)	57.97 (26)	58.14 (33)		
	qB/MHz	2.706 (20)	2.729 (10)	2.731 (13)		
	qD/kHz	1.36 (31)	1.10 (11)	1.10 (15)		
4	E_4/MHz		483299.55 (32)	483299.54 (38)		483301.067 (54)
	B/MHz		5030.558 (23)	5030.566 (29)		5030.494 (13)
	D/kHz		48.79 (17)	48.93 (22)		48.47 (50)
5, 6	$E_{5,6}/\text{MHz}$		734058.59 (30)	729026.77 (37) ^a	734058.62 (39)	
	B/MHz		5031.586 (22)	5031.691 (28)	5031.604	
	D/kHz		48.35 (19)	48.35 (19)	47.70 (39)	
	qB/MHz		12.3861 (73)	12.3862 (91)		
	qD/kHz		-1.191 (74)	-1.176 (92)		
	$B - C^b$					-49.625 (54)
7, 8	$E_{7,8}/\text{MHz}$	2601534.5 (16)	2601533.6 (20)			
	B/MHz	5224.1 (14)	5223.4 (16)			
	D/kHz	72.5 (8)	72.57 (76)			
	qB/MHz	1.7 (13)	2.3 (16)			
	qD/kHz	-77.1 (7)	-77.34 (81)			
9	E_9/MHz	2672389.1 (8)	2672387.7 (8)			
	B/MHz	5292.4 (28)	5293.5 (33)			
	D/kHz	221.1 (15)	222.7 (18)			
	c/MHz	6474 (32)	6460 (39)			
	N	59	148	89		
	σ/MHz	1.2	1.2	0.9		

^a The discrepancies here are due the different energy expressions used in this paper and ref 11. ^b Reference 9 used a different energy expression.

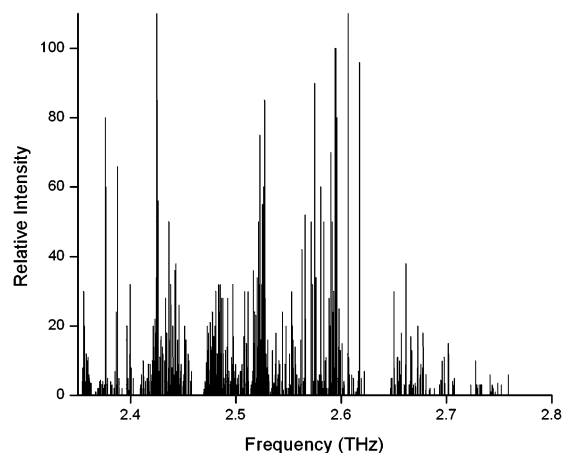


Figure 1. Stick spectrum of entire scanned region. It should be noted that these are composite spectra that include transitions from several laser lines. Only the intensities of transitions from the same laser line are comparable.

interaction is really big also supports the idea that this observed mode involves the out-of-plane twist.

Using their model intermolecular potential, Olthof et al.^{21,22} were able to reproduce all the observed far-infrared ground vibrational state rotation-tunneling states with an accuracy of about 0.25 cm^{-1} ; furthermore, they could model the Coriolis coupling, dipole moments of the $A + E$ states, and the nuclear quadrupole splittings of the $A + E$ states with $K = 0$ and $K = 1$, in good agreement with the experimental data. However, further studies showed the need for further refinement. Karyakin et al.¹⁶ determined the $A + A$ states interchange splitting of $(\text{ND}_3)_2$. Their observed value of 264 GHz is about 25% smaller than the calculated 331 GHz, while the calculated $A + A$ interchange splitting of $(\text{NH}_3)_2$ of 475 GHz matches the experimental value of 483 GHz very well. Heineking et al.¹⁴ studied the nuclear quadrupole coupling of the $E + E$ states with $K = 0$, and compared the experimental values with the

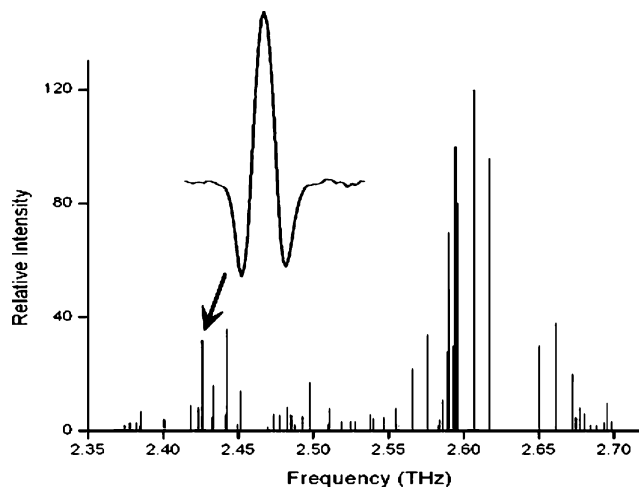


Figure 2. Stick spectrum of the assigned A–A (ortho–ortho) state transitions with a sample spectrum.

ones calculated using the potential Olthof et al. developed. They found that the calculated χ_{aa} agrees well with the experimental value, while there is discrepancy between the calculated and the observed value of $\chi_{bb} - \chi_{cc}$. They concluded that this potential is very accurate in its dependence on the polar angles, but probably too soft in its dependence on the dihedral angle. It would thus be interesting to expand the scanning region to identify the other half of the tunneling levels to ascertain how the interchange is affected by this intermolecular vibration and to improve this potential as it probes the excitations in the dihedral angle. However, it was found that the interchange splitting is about 3 times larger in the $K_a = 0$ of the excited state of water dimer than the value of the ground state, and about 9 times larger for the 4295 GHz subband.⁴¹ Since the interchange splitting for the ammonia dimer is ca. 20 cm^{-1} , the other half of the tunneling levels for this out-of-plane vibration could easily fall outside of the current coverage of our

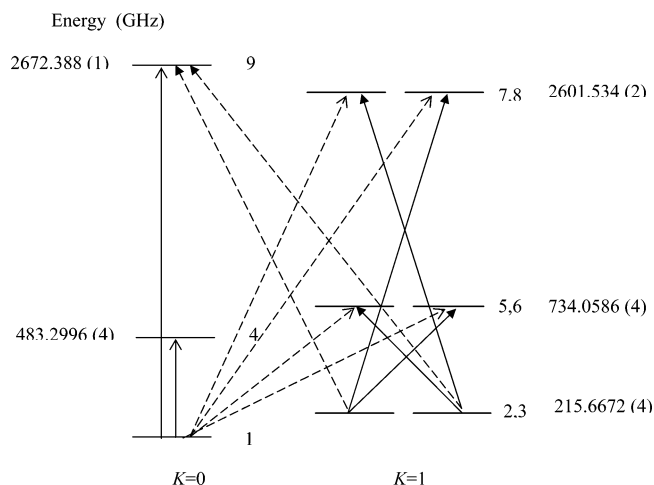


Figure 3. Vibration-rotation-tunneling energy levels for the A-A (ortho-ortho) states of the ammonia dimer. The dashed arrows indicate perpendicular bands, solid arrows correspond to parallel bands. The open arrowheads correspond to transitions from the vibrational ground state and the closed ones to hot band transitions from the $n = 2,3$ levels.

spectrometer, and thus constitutes a major search problem. It would also be interesting to locate the “geared” in-plane bend, as well as the intermolecular stretch vibrations, and such efforts are underway.

Acknowledgment. This work was supported by the Experimental Physical Chemistry Division of the National Science Foundation. We would like to thank Prof. William Klemperer and Prof. Martina Havenith for their helpful comments. W.L. would like to thank Prof. Stewart Novick and Dr. Herbert Pickett for their help with the SPFIT program.

References and Notes

- (1) Nelson, D. D., Jr.; Fraser, G. T.; Klemperer, W. *Science* **1987**, *238*, 1670.
- (2) Nelson, D. D., Jr.; Fraser, G. T.; Klemperer, W. *J. Chem. Phys.* **1985**, *83*, 6201.
- (3) Nelson, D. D., Jr.; Klemperer, W. *J. Chem. Phys.* **1987**, *87*, 139.
- (4) Nelson, D. D., Jr.; Klemperer, W.; Fraser, G. T.; Lovas, F. J.; Suenram, R. D. *J. Chem. Phys.* **1987**, *87*, 6364.
- (5) Pimentel, G. C.; Bulanin, M. O.; Thiel, M. van *J. Chem. Phys.* **1962**, *36*, 500.
- (6) Frisch, M. J.; Bene, J. E. del; Binkley, J. S.; Schaefer, H. F., III. *J. Chem. Phys.* **1986**, *84*, 2279.
- (7) Liu, S.; Dykstra, C. E.; Kolenbrander, K.; Lisy, J. M. *J. Chem. Phys.* **1986**, *85*, 2077.
- (8) Boese, A. D.; Chandra, A.; Martin, J. M. L.; Marx, D. *J. Chem. Phys.* **2003**, *119*, 5965.
- (9) Havenith, M.; Cohen, R. C.; Busarow, K. L.; Gwo, D.-H.; Lee, Y. T.; Saykally, R. J. *J. Chem. Phys.* **1990**, *94*, 4776.
- (10) Havenith, M.; Linnartz, H.; Zwart, E.; Kips, A.; Meulen, J. J. ter; Meerts, W. L. *Chem. Phys. Lett.* **1992**, *193*, 261.
- (11) Loeser, J. G.; Schmuttenmaer, C. A.; Cohen, R. C.; Elrod, M. J.; Steyert, D. W.; Saykally, R. J.; Bumgarner, R. E.; Blake, G. A. *J. Chem. Phys.* **1992**, *97*, 4727.
- (12) Linnartz, H.; Kips, A.; Meerts, W. L.; Havenith, M. *J. Chem. Phys.* **1993**, *99*, 2449.
- (13) Cotti, G.; Linnartz, H.; Meerts, W. L.; van der Avoird, A.; Olthof, E. H. T. *J. Chem. Phys.* **1995**, *104*, 3898.
- (14) Heineking, N.; Stahl, W.; Olthof, E. H. T.; Wormer, P. E. S.; van der Avoird, A.; Havenith, M. *J. Chem. Phys.* **1995**, *102*, 8693.
- (15) Behrens, M.; Buck, U.; Frochtenicht, R.; Hartmann, M.; Havenith, M. *J. Chem. Phys.* **1997**, *107*, 7179.
- (16) Karyakin, E. N.; Fraser, G. T.; Loeser, J. G.; Saykally, R. J. *J. Chem. Phys.* **1999**, *110*, 9555.
- (17) Müller-Dethlefs, K.; Hobza, P. *Chem. Rev.* **2000**, *100*, 143.
- (18) Havenith, M. *Infrared Spectroscopy of Molecular Clusters*; Springer Verlag: Berlin, 2002; Chapter 9.
- (19) Bunker, P. R.; Jensen, P. *Molecular Symmetry and Spectroscopy*, 2nd ed.; NRC Research Press: Ottawa, 1998; p 579.
- (20) Altmann, J. A.; Govender, M. G.; Ford, T. A. *Mol. Phys.* **2005**, *103*, 949 and references therein.
- (21) Olthof, E. H. T.; van der Avoird, A.; Wormer, P. E. S. *J. Chem. Phys.* **1994**, *101*, 8430.
- (22) Olthof, E. H. T.; van der Avoird, A.; Wormer, P. E. S.; Loeser, J. G.; Saykally, R. J. *J. Chem. Phys.* **1994**, *101*, 8443.
- (23) van der Avoird, A.; Olthof, E. H. T.; Wormer, P. E. S. *Faraday Discuss.* **1994**, *97*, 43.
- (24) Keutsch, F. N.; Goldman, N.; Harker, H. A.; Leforestier, C.; Saykally, R. J. *Mol. Phys.* **2003**, *101*, 3477.
- (25) Keutsch, F. N.; Cruzan, J. D.; Saykally, R. J. *Chem. Rev.* **2003**, *103*, 2533.
- (26) Han, J.-X.; Takahashi, L. K.; Lin, W.; Lee, E. Saykally, R. J. *Chem. Phys. Lett.* **2006**, *423*, 344.
- (27) Cruzan, J. D.; Braly, L. B.; Liu, K.; Brown, M. G.; Loeser, J. G.; Saykally, R. J. *Science* **1996**, *271*, 59.
- (28) Harker, H. A.; Viant, M. R.; Keutsch, F. N.; Michael, E. A.; McLaughlin, R. P.; Saykally, R. J. *J. Phys. Chem. A* **2005**, *109*, 6483.
- (29) Leforestier, C.; Gatti, F.; Fellers, R. S.; Saykally, R. J. *J. Chem. Phys.* **2002**, *117*, 8710.
- (30) Goldman, N.; Fellers, R. S.; Brown, M. G.; Braly, L. B.; Keoshian, C. J.; Leforestier, C.; Saykally, R. J. *J. Chem. Phys.* **2002**, *116*, 10148.
- (31) Smit, M. J.; Groenenboom, G. C.; Wormer, P. E. S.; van der Avoird, A.; Bukowski, R.; Szalewicz, K. *J. Phys. Chem. A* **2001**, *105*, 6212.
- (32) Loeser, J. G. *Faraday Discuss. Chem. Soc.* **1994**, *97*, 159.
- (33) Marsden, C. J. Private communication to R.J.S., June 1991.
- (34) Dykstra, C. E.; Andrews, L. *J. Chem. Phys.* **1990**, *92*, 6043.
- (35) Elrod, M. J. Ph.D. Dissertation, University of California at Berkeley, 1994.
- (36) Blake, G. A.; Laughlin, K. B.; Cohen, R. C.; Busarow, K. L.; Gwo, D.-H.; Schmuttenmaer, C. A.; Steyert, D. W.; Saykally, R. J. *Rev. Sci. Instrum.* **1991**, *62*, 1693.
- (37) Blake, G. A.; Laughlin, K. B.; Cohen, R. C.; Busarow, K. L.; Gwo, D.-H.; Schmuttenmaer, C. A.; Steyert, D. W.; Saykally, R. J. *Rev. Sci. Instrum.* **1991**, *62*, 1701.
- (38) Pickett, H. M. *J. Mol. Spectrosc.* **1991**, *148*, 371. The SPCAT and SPFIT spectroscopic predicting and fitting programs are available as free downloads from <http://spec.jpl.nasa.gov/>.
- (39) Linnartz, H.; Meerts, W. L.; Havenith, M. *Chem. Phys.* **1995**, *193*, 327.
- (40) Loeser, J. G.; Ph.D. Dissertation, University of California at Berkeley, 1995.
- (41) Keutsch, F. N.; Braly, L. B.; Brown, M. G.; Harker, H. A.; Petersen, P. B.; Leforestier, C.; Saykally, R. J. *J. Chem. Phys.* **2003**, *119*, 8927.